JACS
JOURNAL OF THE AMERICAN CHEMICAL SOCIETY
Communication
pubs.acs.org/JACS

The Crystalline Structure of Copper Phthalocyanine Films on ZnO(1$\bar{1}$00)

Amy C. Cruickshank,[†] Christian J. Dotzler,[‡,§] Salahud Din,[†] Sandrine Heutz,[†] Michael F. Toney,*[,§] and Mary P. Ryan*[,†]

[†]Department of Materials and London Centre for Nanotechnology, Imperial College London, Exhibition Road, London SW7 2AZ, United Kingdom

[‡]Industrial Research Ltd., P.O. Box 31-310, Lower Hutt 5040, New Zealand

[§]Stanford Synchrotron Radiation Lightsource, SLAC National Accelerator Laboratory, Menlo Park, California 94025, United States

Supporting Information

ABSTRACT: The structure of copper phthalocyanine (CuPc) thin films (5−100 nm) deposited on single-crystal ZnO(1$\bar{1}$00) substrates by organic molecular beam deposition was determined from grazing-incidence X-ray diffraction reciprocal space maps. The crystal structure was identified as the metastable polymorph α-CuPc, but the molecular stacking was found to vary depending on the film thickness: for thin films, a herringbone arrangement was observed, whereas for films thicker than 10 nm, coexistence of both the herringbone and brickstone arrangements was found. We propose a modified structure for the herringbone phase with a larger monoclinic β angle, which leads to intrastack Cu−Cu distances closer to those in the brickstone phase. This structural basis enables an understanding of the functional properties (e.g., light absorption and charge transport) of (opto)electronic devices fabricated from CuPc/ZnO hybrid systems.

Organic small-molecule semiconductors are gaining increasing importance for use in low-cost optoelectronic devices, such as solar cells[1] and field-effect transistors.[2] One promising candidate is the planar π-conjugated molecule copper(II) phthalocyanine (CuPc) (Figure 1a),[3,4] which was one of the first organic semiconductors discovered.[5] However, despite its long history, information about the structural properties of CuPc remains incomplete, even though knowledge of the molecular orientation and ordering[6,7] is important for achieving high-performance electronic devices.

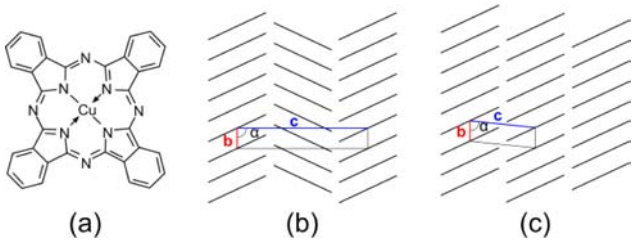

Figure 1. (a) Structure of the CuPc molecule. (b, c) Schematics of the (b) herringbone[8] and (c) brickstone[9] structures of α-CuPc. The views along a^* of the (b) monoclinic and (c) triclinic unit cells are indicated.

CuPc has been shown to form a variety of polymorphs, with the most commonly observed crystal phases being the α and β polymorphs.[8−10] In contrast to the well-characterized structure of the stable β-CuPc polymorph,[10] controversy still exists regarding the structure of metastable α-CuPc (the most common phase grown at deposition temperatures below 200 °C)[11−14] because large enough single crystals have not been formed successfully, and therefore, powder and thin-film diffraction have yielded only limited structural information.[9] Consequently, the thin-film structure of α-CuPc has been variously reported as monoclinic,[8] triclinic,[9] tetragonal,[15] and orthorhombic.[16] While most authors reference the monoclinic structure (space group $C2/c$) by Ashida et al.,[8] in which the molecular stacking arrangement adopts a herringbone structure (Figure 1b), a recent reinvestigation of films prepared according to Ashida's original work by Hoshino et al.[9] came to the conclusion that the molecular arrangement of α-CuPc must adopt a brickstone arrangement with a triclinic crystal structure (Figure 1c). All of these interpretations were based on electron diffraction measurements performed on 300 nm thick CuPc films.

One example of the use of CuPc in optoelectronic devices is the fabrication of photovoltaic devices consisting of CuPc as a strongly absorbing organic donor material and an inorganic metal oxide (e.g., ZnO) as an electron acceptor/transport layer. These hybrid CuPc/ZnO structures offer an attractive strategy for the production of low-cost solar cells; however, the functional properties and performance of these devices depend strongly on the interface characteristics and structural arrangement of the two materials, which are poorly understood.

In this paper, we describe changes in the structure and molecular ordering of CuPc films (5−100 nm thick) deposited on nonpolar single-crystal ZnO(1$\bar{1}$00) substrates at room temperature, which were examined using grazing-incidence X-ray diffraction (GIXD). Thickness-dependent reciprocal space maps (RSMs), which allow in-plane and out-of-plane lattice properties of the CuPc films to be resolved, revealed that the crystal structure for our CuPc films is the metastable α-CuPc polymorph; however, depending on the film thickness, the CuPc molecules adopt either a purely herringbone arrangement (very thin films) or a combination of herringbone and brickstone

Received: June 13, 2012
Published: August 16, 2012

dx.doi.org/10.1021/ja305760b | J. Am. Chem. Soc. 2012, 134, 14302−14305

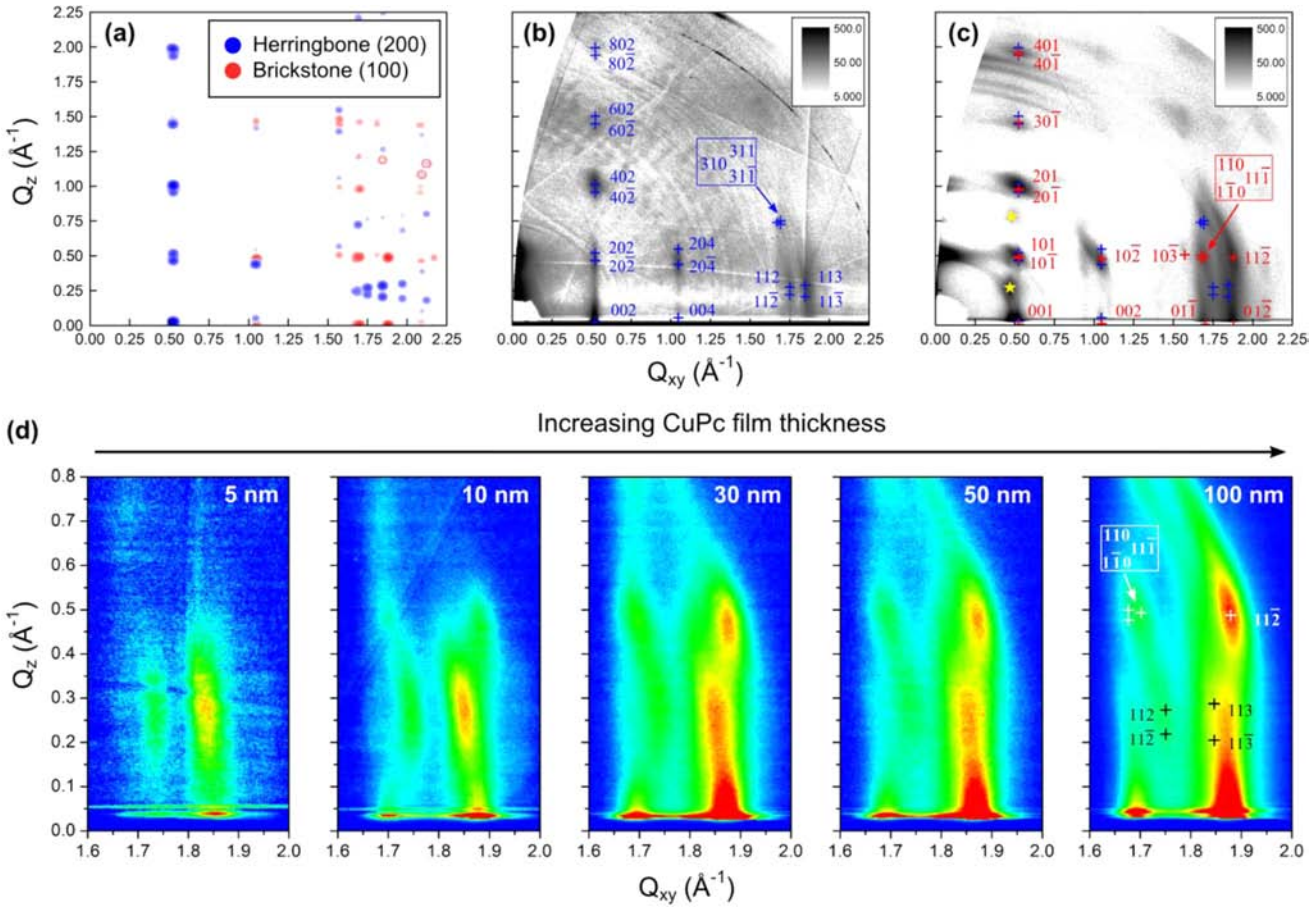

Figure 2. RSMs for α-CuPc. (a) Simulated peak positions for the (200)-oriented herringbone structure[8] (blue symbols; monoclinic crystal system with four molecules per unit cell and lattice parameters a = 25.92 Å, b = 3.79 Å, c = 23.92 Å, β = 90.4°) and the (100)-oriented brickstone structure[9] (red symbols; triclinic crystal system with one molecule per unit cell and lattice parameters a = 12.886 Å, b = 3.769 Å, c = 12.061 Å, α = 96.22°, β = 90.62°, γ = 90.32°). (b, c) RSMs for CuPc films with thicknesses of (b) 5 nm and (c) 100 nm on ZnO($1\bar{1}00$) substrates obtained from GIXD patterns, with high-intensity peaks indexed for the modified (200)-oriented herringbone structure (blue symbols) and the (100)-oriented brickstone structure[9] (red symbols). (d) Selected region of the RSMs for films with increasing CuPc thickness. Main peaks of interest are indicated in the far-right image for the (100)-oriented brickstone structure[9] (white symbols) and the modified (200)-oriented herringbone structure (black symbols).

arrangements (films thicker than 10 nm). Furthermore, we propose a modified structure for the herringbone phase with a larger monoclinic β angle and intrastack Cu−Cu distances closer to those in the brickstone phase. This modified structure provides a stronger basis for understanding the properties of CuPc/ZnO devices, such as light absorption and charge transport.

CuPc films with nominal thicknesses of 5, 10, 30, 50, and 100 nm were deposited on ZnO($1\bar{1}00$) substrates (Pi-Kem Ltd.) by organic molecular beam deposition (OMBD) using a Kurt J. Lesker ultrahigh vacuum chamber with a base pressure of 5 × 10^{-8} mbar. The ZnO substrates were used as received. CuPc powder (Aldrich, 97% purity) was also used as received and evaporated at nominal growth rates of 0.1 Å s^{-1} for 5 and 10 nm films and 1 Å s^{-1} for 30, 50, and 100 nm films, onto the ZnO substrates held at room temperature. The thicknesses of the films were monitored in situ using calibrated quartz crystal microbalances situated near the substrates. GIXD measurements were performed at beamline 11-3 of the Stanford Synchrotron Radiation Lightsource. The X-ray energy was fixed at 12.7 keV. For each sample, diffraction information was collected from the entire CuPc film thickness by selecting incidence angles of 0.15−0.2°, which are slightly below the critical angle of total external reflection of ZnO (0.21°) but above that of CuPc (0.12°). Scattered X-rays were detected using a MAR 345 image-plate area detector. The raw two-dimensional (2D) intensity data were corrected for polarization and geometrical aberrations and translated into an RSM (Q_z vs Q_{xy} plot) using WxDiff.[17] This software was also used to determine the (Q_{xy}, Q_z) coordinates of the peaks and to subtract background scattering from the regions of interest in the RSM for the extraction of diffraction peak intensities and for visualization. Simulations of 2D diffraction patterns were performed using the SimDiffraction software package.[18] For the calculations, crystallographic information files (CIFs) published in the Cambridge Crystallographic Data Centre were used. Lorentz corrections, polarization corrections, and Debye−Waller factors were included in the simulations. UV/vis absorption spectra were recorded using a PerkinElmer Lambda 25 UV/vis spectrometer.

Figure 2a shows a simulated RSM indicating the peak positions for the two most commonly referenced crystal structures of α-CuPc. The blue symbols represent peaks corresponding to the (200)-oriented herringbone structure[8] based on a monoclinic crystal system, and the red symbols represent the (100)-oriented brickstone structure[9] with a triclinic crystal system. Figure 2a shows that while peaks corresponding to the herringbone and brickstone phases overlap along the Q_z direction at Q_{xy} = 0.52 and 1.04 Å^{-1}, they differ in the region between Q_{xy} = 1.7 and 1.9

dx.doi.org/10.1021/ja305760b | J. Am. Chem. Soc. 2012, 134, 14302−14305

$Å^{-1}$; therefore, this region was used to distinguish which stacking arrangement the CuPc molecules adopt in films deposited on ZnO(1$\bar{1}$00) substrates. It is noted that the overall intensities in Figure 2a were scaled for better visibility and do not claim to reproduce the experimentally observed RSMs (Figure 2b,c) quantitatively.

Figure 2b,c shows RSMs obtained for 5 and 100 nm thick CuPc films deposited on ZnO(1$\bar{1}$00). The 5 nm film exhibits several strong peaks at Q_{xy} = 0.52 and 1.04 $Å^{-1}$ that have a streaked shape along Q_z, as expected for a thin film with a high degree of crystallographic texture. The Q_z positions of the peaks coincide approximately with multiples of 0.5 $Å^{-1}$. Additionally, there are two broad features at $Q_z \approx 0.27$ $Å^{-1}$ between Q_{xy} = 1.7 and 1.9 $Å^{-1}$. Comparison with the simulated RSM in Figure 2a shows that the peaks observed along Q_{xy} = 0.52 and 1.04 $Å^{-1}$ in Figure 2b for the 5 nm film can be indexed on the basis of either the (100)-oriented brickstone structure[9] or the (200)-oriented herringbone structure[8]. For both of these structural arrangements, the CuPc molecules do not lie flat on the ZnO (1$\bar{1}$00) surface. Instead, the CuPc molecular plane is tilted 81.87° and 87.92° with respect to the ZnO(1$\bar{1}$00) surface for the brickstone[9] and herringbone[8] structures, respectively. By contrast, the peaks at Q_{xy} = 1.7−1.9 $Å^{-1}$, $Q_z \approx 0.27$ $Å^{-1}$ in Figure 2b can be assigned only to the herringbone structure, demonstrating that the 5 nm CuPc films consist of a highly (200)-textured, purely herringbone structure. Upon closer examination of the (Q_{xy}, Q_z) peak positions observed between Q_{xy} = 1.7 and 1.9 $Å^{-1}$ for the 5 nm CuPc films, it was found that these were slightly shifted relative to those calculated from the herringbone model proposed by Ashida et al.[8] (Table 1). Calculating the lattice parameters from the peak positions in Figure 2b gave a = 25.6 Å, b = 3.76 Å, c = 24.0 Å, β = 93° (see the Supporting Information for the CIF).

Table 1. Comparison of the (Q_{xy}, Q_z) Coordinates of the (112) and (113) Peaks for the 5 nm CuPc Film on ZnO(1$\bar{1}$00) with Those Calculated for the α-CuPc Herringbone Structures Proposed by Ashida et al.[8] and in This Work

	5 nm film on ZnO(1$\bar{1}$00)		α-herringbone (ref 8)		α-herringbone (this work)	
reflection	Q_{xy} ($Å^{-1}$)	Q_z ($Å^{-1}$)	Q_{xy} ($Å^{-1}$)	Q_z ($Å^{-1}$)	Q_{xy} ($Å^{-1}$)	Q_z ($Å^{-1}$)
112	~1.76	~0.27	1.74	0.25	1.75	0.27
11$\bar{2}$			1.74	0.24	1.75	0.22
113	~1.86	~0.29	1.84	0.25	1.85	0.29
11$\bar{3}$			1.84	0.24	1.85	0.20

Our new proposed herringbone structure leads to a larger splitting between the (112)/(11$\bar{2}$) and (113)/(11$\bar{3}$) peaks compared with the model proposed by Ashida et al.[8] (Table 1). While this splitting was not visible for the thin films used here because of the low intensity of the 11$\bar{2}$ /11$\bar{3}$ peaks, it could be used to identify this phase in thicker materials. It is also noted that our new proposed herringbone structure leads to a small change in the CuPc tilt angle with respect to the ZnO(1$\bar{1}$00) surface (86.82°) compared with that predicted by the model proposed by Ashida et al.[8] (87.92°).

In comparison to the 5 nm CuPc films on ZnO(1$\bar{1}$00), the 100 nm films exhibited peaks at approximately similar positions, but several additional overlapping peaks were also observed (compare panels b and c in Figure 2). In the region Q_{xy} = 1.7−1.9 $Å^{-1}$, peaks corresponding to the herringbone phase were observed at $Q_z \approx 0.27$ $Å^{-1}$, but additional strong peaks were also observed at Q_z = 0 and 0.5 $Å^{-1}$ (Figure 2c for 100 nm CuPc). Comparison with the simulated RSM shown in Figure 2a revealed that while the peaks at Q_z = 0 and 0.5 $Å^{-1}$ are absent in the herringbone model, they are present in the brickstone model. Hence, thicker films exhibit *both* the herringbone and brickstone structures. It is noted that the peaks observed in Figure 2c are indexed according to both the herringbone structure from this work (blue crosses) and brickstone structure (red crosses). We also note in Figure 2c that there are two additional reflections at $Q_{xy} \approx 0.48$ $Å^{-1}$ and $Q_z \approx 0.27$ and 0.78 $Å^{-1}$ (yellow stars) for which neither of the two morphologies can account. Their origin is the subject of further investigation but may be due to a more complex structure.

To investigate further the change in structure with increasing CuPc film thickness, the RSM between Q_{xy} = 1.6 and 2.0 $Å^{-1}$ was plotted for film thicknesses of 5, 10, 30, 50, and 100 nm (Figure 2d). The intensity scaling was normalized to ensure that the regions consisting of the (112) and (113) peaks of the herringbone structure (indicated by black symbols) appear with similar intensities for all thicknesses. This demonstrates the *relative* increase in intensity for the peaks characteristic of the brickstone structure (white symbols) with respect to the herringbone structure as the CuPc film thickness increases. Figure 2d shows that the 5 nm film is dominated by the herringbone structure, while films with thicknesses of 10−100 nm all exhibit both the herringbone and brickstone structures. We note that the transition in structure occurs at a film thickness of 10 nm in the slow-growth regime (0.1 Å s^{-1}). This trend is continued for thicker films grown at a higher growth rate (1 Å s^{-1}). The observed coexistence of herringbone and brickstone structures is in remarkable contrast to the findings by Hoshino et al.,[9] who concluded from electron diffraction data that films of CuPc deposited on KCl substrates *always* adopt a brickstone configuration and assigned this structure to the α-polymorph. However, the coexistence of herringbone and brickstone structures for ultrathin films was suggested in early work by Kobayashi et al.[19] on the basis of transmission electron microscopy examination of CuPc films deposited on KCl substrates.

It is likely that the coexistence of the herringbone and brickstone configurations in the thicker films is due to strong interactions between molecules *within* a column but relatively weak interstack interactions. Figure 3 summarizes the relative orientations of two neighboring molecules within the molecular stack for the known α and β phases in comparison with our proposed structure for the thin-film herringbone phase. Here we notice that while our structure follows that usually associated with herringbones (as defined by Hoshino et al.[9]), the interplanar

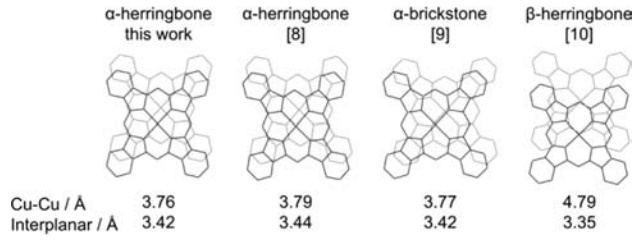

Figure 3. Projections of two molecules in a column parallel to their molecular planes. Cu−Cu distances (corresponding to the crystallographic b axis) and interplanar distances between molecular planes are also listed.

dx.doi.org/10.1021/ja305760b | J. Am. Chem. Soc. 2012, 134, 14302−14305

spacing and the Cu−Cu distance are more similar to those of the brickstone model. Therefore, although both the herringbone and brickstone structures coexist in our thicker films, the interplanar spacing and Cu−Cu distance do not depend on the thickness. These quantities dominate important physical properties, such as charge transport,[20] light absorption,[21] and magnetism,[22] and our new structure could rationalize why other authors have observed these physical properties to be independent of thickness. Figure 4

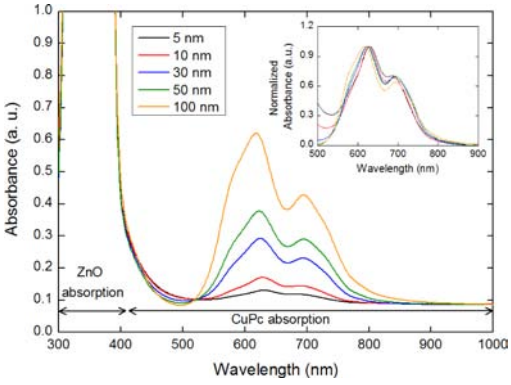

Figure 4. UV/vis absorption spectra of α-CuPc films with increasing film thickness deposited on ZnO($1\bar{1}00$) substrates. The inset shows normalized absorption spectra exhibiting small wavelength shifts for the absorption bands as the film thickness is varied.

presents UV/vis absorption spectra for CuPc films deposited on ZnO($1\bar{1}00$) with increasing film thicknesses between 5 and 100 nm. The intensity of the light absorbed scaled with the film thickness, and very small wavelength shifts are observed for the absorption bands. The wavelength shift is attributed to the incorporation of CuPc molecules arranged in a brickstone structure into the film. The small extent of the wavelength shift is most likely due to the similarities of the CuPc molecular spacings and tilt angles on the ZnO($1\bar{1}00$) surface for the herringbone and brickstone structures.

In conclusion, we have observed a high degree of orientation in CuPc films with thicknesses of 5−100 nm grown by OMBD on single-crystal ZnO($1\bar{1}00$) substrates. The crystal structure of the films was α-CuPc but occurred in at least two different modifications depending on the thickness. Films with thicknesses below ∼10 nm were dominated by a herringbone arrangement of the molecular stacks with slight modifications of the structure reported by Ashida et al.,[8] whereas thicker films increasingly contained a polymorph with a brickstone arrangement similar to the structure reported by Hoshino et al.[9] The modified herringbone structure proposed in this work, with a larger monoclinic β angle and intrastack Cu−Cu distances similar to those in the brickstone phase, will likely have a major influence on the functional properties of (opto)electronic devices fabricated from CuPc/ZnO hybrid structures, and an understanding of this behavior is vital for the design and optimization of new hybrid device architectures.

■ ASSOCIATED CONTENT

Ⓢ Supporting Information

Crystallographic data for the proposed modified herringbone structure of α-CuPc (CIF). This material is available free of charge via the Internet at http://pubs.acs.org.

■ AUTHOR INFORMATION

Corresponding Author

mftoney@slac.stanford.edu; m.p.ryan@imperial.ac.uk

Notes

The authors declare no competing financial interest.

■ ACKNOWLEDGMENTS

A.C.C. and M.P.R. gratefully acknowledge the U.K. Engineering and Physical Sciences Research Council (EPSRC) for financial support (Nanotechnology Grand Challenge Grants EP/F056362/1 and EP/F056184/1). C.J.D. and M.P.R. acknowledge financial support from the New Zealand Foundation for Research, Science and Technology (CO8X0409). S.D. and S.H. thank Kurt J. Lesker and EPSRC for the award of a CASE studentship. S.H. thanks EPSRC for grants EP/F039948/1 and EP/F04139X/1. Portions of this research were carried out at the Stanford Synchrotron Radiation Lightsource, a Directorate of the SLAC National Accelerator Laboratory and an Office of Science User Facility operated for the U.S. Department of Energy Office of Science by Stanford University.

■ REFERENCES

(1) Riede, M.; Mueller, T.; Tress, W.; Schueppel, R.; Leo, K. *Nanotechnology* **2008**, *19*, No. 424001.
(2) Zeis, R.; Siegrist, T.; Kloc, Ch. *Appl. Phys. Lett.* **2005**, *86*, No. 022103.
(3) de Boer, R. W. I.; Gershenson, M. E.; Morpurgo, A. F.; Podzorov, V. *Phys. Status Solidi A* **2004**, *201*, 1302.
(4) Wöhrle, D.; Kreienhoop, L.; Schlettwein, D. In *Phthalocyanines: Properties and Applications*; Leznoff, C. C., Lever, A. B. P., Eds.; VCH: New York, 1996; Vol. *4*, p 219.
(5) Vartanyan, A. T. *Zh. Fiz. Khim.* **1948**, *22*, 769.
(6) Sylvester-Hvid, K. O. *J. Phys. Chem. B* **2006**, *110*, 2618.
(7) Cheng, C. H.; Wang, J.; Du, G. T.; Shi, S. H.; Du, Z. J.; Fan, Z. Q.; Bian, J. M.; Wang, M. S. *Appl. Phys. Lett.* **2010**, *97*, No. 083305.
(8) Ashida, M.; Uyeda, N.; Suito, E. *Bull. Chem. Soc. Jpn.* **1966**, *39*, 2616.
(9) Hoshino, A.; Takenaka, Y.; Miyaji, H. *Acta Crystallogr.* **2003**, *B59*, 393.
(10) Brown, C. J. *J. Chem. Soc. A* **1968**, 2488.
(11) Tokito, S.; Sakata, J.; Taga, Y. *Thin Solid Films* **1995**, *256*, 182.
(12) Maggioni, G.; Quaranta, A.; Carturan, S.; Patelli, A.; Tonezzer, M.; Ceccato, R.; Della Mea, G. *Chem. Mater.* **2005**, *17*, 1895.
(13) E, J.; Kim, S.; Lim, E.; Lee, K.; Cha, D.; Friedman, B. *Appl. Surf. Sci.* **2003**, *205*, 274.
(14) Prabakaran, R.; Kesavamoorthy, R.; Reddy, G. L. N.; Xavier, F. P. *Phys. Status Solidi B* **2002**, *229*, 1175.
(15) Robinson, M. T.; Klein, G. E. *J. Am. Chem. Soc.* **1952**, *74*, 6294.
(16) Assour, J. M. *J. Phys. Chem.* **1965**, *69*, 2295.
(17) Mannsfield, S. C. B. *WxDiff*; Stanford Synchrotron Radiation Lightsource: Menlo Park, CA; http://code.google.com/p/wxdiff.
(18) Breiby, D. W.; Bunk, O.; Andreasen, J. W.; Lemke, H. T.; Nielsen, M. M. *J. Appl. Crystallogr.* **2008**, *41*, 262.
(19) Kobayashi, T.; Fujiyoshi, Y.; Uyeda, N. *Acta Crystallogr.* **1982**, *A38*, 356.
(20) Dimitrakopoulos, C. D.; Malenfant, P. R. L. *Adv. Mater.* **2002**, *14*, 99.
(21) Fronk, M.; Zahn, D. R. T.; Salvan, G. *Phys. Status Solidi C* **2010**, *7*, 214.
(22) Heutz, S.; Mitra, C.; Wu, W.; Fisher, A. J.; Kerridge, A.; Stoneham, M.; Harker, T. H.; Gardener, J.; Tseng, H. H.; Jones, T. S.; Renner, C.; Aeppli, G. *Adv. Mater.* **2007**, *19*, 3618.